The Architecture of the Binding Site in Redox Protein Complexes: Implications for Fast Dissociation

Peter B. Crowley* **and Maria Arménia Carrondo**
Instituto de Tecnologia Química e Biológica, Universidade Nova de Lisboa, Av. Da República, Apartado 127, 2781 901 Oeiras, Portugal

ABSTRACT **Interprotein electron transfer is characterized by protein interactions on the millisecond time scale. Such transient encounters are ensured by extremely high rates of complex dissociation. Computational analysis of the available crystal structures of redox protein complexes reveals features of the binding site that favor fast dissociation. In particular, the complex interface is shown to have low geometric complementarity and poor packing. These features are consistent with the necessity for fast dissociation since the absence of close packing facilitates solvation of the interface and disruption of the complex. Proteins 2004;55:603–612.**

Key words: atom packing; crystal structure; electron transfer; protein interactions; recognition

INTRODUCTION

Biological electron transfer is performed by proteins, which contain cofactors specialized for controlled redox behavior.[1] Redox proteins have two primary functions: to insulate and fine-tune the redox center and to recognize reaction partners in the cell. Discrimination between partners and other proteins in the cellular environment can be achieved when the maximum lowering of the system free energy occurs upon binding to the specific partner. Due to the complex nature of their surfaces, however, protein recognition remains poorly understood.

Depending on the lifetime and the affinity of the complex, protein interactions can be broadly classified as either static or transient. The interaction of barnase (an extracellular endonuclease) and barstar (an intracellular inhibitor of barnase), with a dissociation constant (K_d) of $\sim 10^{-14}$ M, is a well-studied example of a static complex.[2] This highly specific and long-lived complex has evolved in order to thoroughly block the intracellular activity of barnase, thereby protecting the host. In contrast to static complexes, transient complexes are characterized by short lifetimes and weak binding affinities. Such features are required by high-turnover systems as found in electron transfer chains, which demand a continuous flow of electrons.[1,3] Although adequate to permit electron transfer, the lifetime of the interaction must not prohibit product dissociation and turnover. Fast rates of complex dissociation (e.g., $k_{off} > 10^2$ s^{-1}) enable such transient interactions. Typically, with shorter lifetimes and lower affinities, the capacity to form highly specific complexes decreases.[4] This is favorable because redox proteins transport electrons between at least two components of the chain and therefore use binding sites, which must be sufficiently responsive toward different molecular surfaces.[5]

Computational analyses of the crystal structures of protein complexes have led to considerable developments in the understanding of protein interactions and recognition.[6–15] Several criteria for categorizing protein complexes, including the interface size, conformation changes, intermolecular polar interactions, atom packing, and geometric fitting, have emerged from this work. At present, the majority of protein complexes reported in the Protein Data Bank[16] (PDB) are of high affinity. Given the difficulty of cocrystallization, transient complexes are poorly represented in the PDB. One such complex, between cytochrome *c* and its peroxidase, was included in a study of 75 complexes by Lo Conte et al.[13] The interface in this complex was found to be an exception because it is small and poorly packed and contains only one hydrogen bond. This observation prompted the authors to conclude that such characteristics may be pertinent to redox protein interactions.[13,17]

In order to investigate this hypothesis, we have applied an interface analysis to all redox protein complexes, including crosslinked complexes, of known structure (Table I).[18–37] Although the interface size correlates poorly with the binding affinity, it is shown that the degree of atom packing is consistently low. This feature is likely to favor both fast dissociation and the promiscuous nature of these complexes. Furthermore, it is shown that, although electrostatic interactions are often important for redox protein

Abbreviations: Ab, *Anabaena*; *adr*, bovine adrenodoxin reductase; *adx*, bovine adrenodoxin; *ami*, *Paracoccus* amicyanin; ASA, accessible surface area; *azu*, *Pseudomonas* azurin; b*, *Bacillus* barstar; bc_1, yeast cytochrome bc_1 complex; br, *Bacillus* barnase; *ccp*, yeast cytochrome *c* peroxidase; *cytc*, yeast cytochrome *c*; $cytc_2$, *Rhodobacter* cytochrome c_2; $cytc_{551}$, *Paracoccus* cytochrome c_{551}; *etf*, *Methylophilus* electron transferring flavoprotein; *fdx*, ferredoxin; *fnr*, ferredoxin $NADP^+$ reductase; *hcytc*, horse heart cytochrome *c*; *madh*, *Paracoccus* methylamine dehydrogenase; Mz, maize; PDB, Protein Data Bank; *rc*, *Rhodobacter* reaction center; *tmadh*, *Methylophilus* trimethylamine dehydrogenase

Grant sponsor: Marie Curie Foundation, Fifth Framework Programme; Grant number: HPMF-CT-2002-02008.

*Correspondence to: P.B. Crowley. E-mail: crowley@itqb.unl.pt

Received 10 September 2003; Revised 27 October 2003; Accepted 7 November 2003

Published online 5 March 2004 in Wiley InterScience (www.interscience.wiley.com). DOI: 10.1002/prot.20043

TABLE I. Redox Protein Complexes

Complex	K_d (μM)	Ref.	PDB	Ref.	Res. (Å)
adx:adr	0.02	18	1e6e	19	2.3
Mz *fdx:fnr*	3	20	1gaq	21	2.6
Ab *fdx:fnr*	2	22	1ewy	23	2.4
ami:madh	4	24	2mta	25	2.4
$cytc_2$*:rc*	1	26	119b	27	2.4
cytc:ccp	5	28	2pcc	29	2.3
hcytc:ccp	1	30	2pcb	29	2.8
azu:azu	—	—	1jvl	31	2.0
etf:tmadh	5	32	1o94	33	2.0
$cytc:bc_1$	0.1	34	1kyo	35	3.0
$ami:cytc_{551}$	20	36	2mta	25	2.4
*br:b**	10^{-8}	2	1brs	37	2.0

All of the known structures of redox protein complexes were analyzed. Two of the complexes, *adx:adr*[19] and the *azu* homodimer,[31] contain covalent crosslinks. The barnase–barstar complex (*br:b**) is an example of a high-affinity static complex,[2] and it was included in the analysis for the purposes of comparison. The equilibrium dissociation constants (K_d) are approximate and should be interpreted with caution considering the strong ionic strength dependence of complex formation.

association, charged groups are rarely involved in interfacial contacts.

MATERIALS AND METHODS

Structure Files

The coordinates for all of the protein complexes were obtained from the PDB.[16] The PDB files were edited as necessary prior to performing any calculations. In cases where several copies of the structure were present in the file, a single copy was retained for calculations. Coordinates of small molecules from the crystallization conditions were also discarded.

Interface Areas

The solvent accessible surface area (ASA) was calculated using the program NACCESS.[38] A probe radius of 1.4 Å was used, and the interface area (B) was defined as the sum of the ASAs of the individual proteins minus the ASA of the complex. The B values were rounded to the nearest 10 Å^2. Interface atoms were identified as those atoms that lose ≥0.05 Å^2 of surface area between the free and bound forms.[14]

Polar Interactions

Hydrogen bonds were identified using the program HBPLUS[39] and the standard geometric criteria for defining hydrogen bonds.[39]

Volume Calculations and Geometric Fitting

The atom volumes and packing efficiency were calculated using an implementation of the Voronoi procedure[40] in a software package developed by Gerstein and coworkers[41] (available at http://www.molmovdb.org/geometry/). The gap volume index was calculated using Surfnet.[42]

RESULTS AND DISCUSSION

Interface Size and Conformation Changes

The size of a protein binding site can be calculated from the difference in the solvent ASAs of the isolated protein and the protein in complex.

Such a calculation identifies all surface atoms, which lose surface accessibility in the complex. Although this procedure measures the area of the protein, which is intimately associated with the interaction, it describes an area much larger than is involved in interfacial contacts. Table II lists the interface area B calculated for each of the complexes. The value indicated is the sum of the two components of the complex, with each component contributing approximately equally. Despite the similarity of function (electron transfer), there is a remarkable variability in the interface size. It should be noted that the size of an interface does not correlate with the size of the proteins involved.[13] Table II includes the smallest known interfaces (800–900 Å) found in two different *cyt* complexes, as well as the large interface found in *adx:adr* (~2300 Å). Four of the complexes have standard-size interfaces (~1600 ± 400 Å). It is apparent from a comparison of Tables I and II that the binding affinity is not linearly dependent on the interface size. One difficulty with such an analysis, however, is the availability of accurate binding constants for each complex. It has been shown that, in general, smaller binding sites have lower binding affinities.[9,15] On this basis it was proposed that each monomer must bury a minimum of ~600 Å^2 in order to have a stable complex.[12] However, the results in Table II indicate that even smaller interfaces exist; *ami*, for example, contributes as little as 400 Å^2 to the complex interface with $cytc_{551}$.

Conformation changes arising from complex formation can be readily identified by comparing the structures of the free and bound forms of the protein. Apart from small rearrangements of side chains and/or loops, conformation changes are uncommon in complexes with small or standard size interfaces.[13] Of the complexes presented in Table I, significant rearrangements have been observed in several cases. In $cytc_2$*:rc*, a tyrosine side chain of *rc*, is displaced by ~2 Å, resulting in the formation of a cation–π interaction with an arginine on $cytc_2$.[27] Similar conformation changes are observed in the *fdx:fnr* complexes. In the maize complex (Mz *fdx:fnr*) a loop movement of *fnr* is compensated by the formation of electrostatic interactions[21] whereas in the *Anabaena* complex (Ab *fdx:fnr*) a loop movement (2.5 Å) in *fdx* is stabilized by hydrophobic interactions.[23] A large conformation change is observed in the *adx:adr* complex where a domain rotation in *adr* accompanies complex formation.[19] Such conformation changes are typical in complexes with large interfaces[13]; however, a similar domain rotation is also observed in the Mz *fdx:fnr* complex.[21] An extreme case of conformational changes has been observed in the *etf:tmadh* complex. On the basis of crystallographic and X-ray scattering data, Leys et al. have reported that the redox active domain of *etf* explores various conformations within the complex interface.[33] Although the structure was included in this

TABLE II. Interface Size, Hydrophobicity, and Polar Interactions in Redox Protein Interfaces

Complex	Interface B (Å^2)	Class[a]	% B Apolar[b]	H Bonds[c] N_{HB}	Cation–π	Most buried residues[d]
adx:adr	2320	Large	51:61	10 (3)	—	**D79:R240**
Mz *fdx:fnr*	1700	Std.	42:59	3 (2)	—	Y37:K91
Ab *fdx:fnr*	1660	Std.	50:50	—	—	S64:R264
ami:madh	1460	Std.	81:67	—	1	F97:P145
cytc$_2$:rc	1270	Std.	57:54	4	1	T101:L191
cytc:ccp	1150	Small	63:48	1	—	**R13:Y39**
hcytc:ccp	1030	Small	66:44	2 (1)	—	**Q12:Y39**
azu:azu	1000	Small	83:83	—		M64:M64
etf:tmadh	960	Small	71:44	3	—	**L194:Y478**
cytc:bc$_1$	870	Small	71:64	—	1	**R13:F230**
ami:cytc$_{551}$	830	Small	63:60	3 (1)	1	**E31:Y77**
Mean	1300 (450)	—	61 (12)	—	—	—
*br:b**	1560	Std.	54:56	13 (3)	—	**R59:D35**
LC Mean	1940 (760)	—	56 (6)	—	—	—

[a]The complexes are classed in terms of the interface size (B) using the criteria of Lo Conte et al.[13]: large $>$ 2000 Å^2, standard = 1600 ± 400 Å^2, small $<$ 1200 Å^2.
[b]The percentage of the interface area composed of apolar atoms. Individual entries correspond to the hydrophobic content of each component of the complex.
[c]Intermolecular hydrogen bonds were calculated using the program HBPLUS.[39] The number of salt bridges is indicated in parentheses.
[d]The residues that contribute the most surface area to the interface are indicated. Those pairs of side chains that make van der Waals contact across the interface are highlighted in bold. For example, in the *adx:adr* complex, D79 of *adx* and R240 of *adr* are the most buried and are in van der Waals contact.
[e]The mean (standard deviation) as calculated for the 11 redox protein complexes.
[f]The mean (standard deviation) from the study by Lo Conte et al.[13] on a set of 75 protein complexes.

study, it should be noted that the interface is incomplete, lacking coordinates for the redox domain of *etf*.

Interface Character and Residue Enrichment

By analyzing the percentage area contributions of amino acids found in protein–protein interfaces, it is possible to observe trends in the interface composition and identify residues types that are important for the interaction.

The gross composition of the interface can be classified in terms of hydrophobicity. Table II lists the percentage area contribution of apolar atoms to the interfaces found in redox protein complexes. On average the interface is more hydrophobic (61% apolar) than the average hydrophobicity (57% apolar) of the solvent-accessible surface of the free proteins (calculated for soluble proteins only). In their study of 75 protein complexes, Lo Conte et al. found the average interface to be 56% apolar.[13] Two of the interfaces have a considerably higher hydrophobic content than the average (Table II). The *azu* homodimer and the *ami:madh* interfaces are 83 and 74% hydrophobic, respectively. This high content of apolar atoms can be attributed to the hydrophobic patch, which is conserved in cupredoxins[43] and mediates protein interactions in this family.[25,31,44,45] Such apolar interfaces are not limited, however, to complexes involving cupredoxins. Although conserved lysine residues have been the traditional focus of research in *cytc* interactions, the binding site is in fact predominantly apolar. The binding sites utilized by the five *c*-type cytochromes (Table II) have an average hydrophobic content of 63%.

Contrary to what might be expected, the hydrophobic content is not always equally divided between the two components of the interface (Table II). For example, in the *cytc:ccp* complex, *cytc* uses a binding site that is 63% hydrophobic and the binding site of the peroxidase is only 48% hydrophobic. It is interesting that the two complexes involving yeast *cytc* differ significantly in terms of the hydrophobic contribution to the interface. When bound to the *cytc$_1$* subunit of the *bc$_1$* complex, *cytc* uses a binding site that is 71% hydrophobic compared to 63% in the peroxidase complex. Similar variations in chemical character are observed in the *fdx:fnr* complexes. In the Maize complex, *fnr* is approximately 10% more apolar and *fdx* approximately 10% more polar than the homologous binding sites in *Anabaena*.

Although the difference in the interface hydrophobicity of redox complexes and the complexes studied by Lo Conte et al.[13] can be considered statistically insignificant, there is an obvious distinction in the amino acid content of the different interfaces. Figure 1 illustrates the percentage area contributions of individual amino acids to the interfaces found in the electron transfer complexes. The results of Lo Conte et al.[13] are included in the plot for comparison. Seven residues have similar percentage area contributions in the two sets of complexes. The charged residues aspartic acid, glutamic acid, and lysine make considerably larger contributions to redox protein complexes; in particular, lysine is twice as frequent. Of the polar side chains, threonine and asparagine contribute almost equally to the two types of interfaces whereas glutamine is more abundant and serine less abundant in redox protein interfaces. Notable differences for hydrophobic residues include alanine, which contributes three times more surface area to redox protein interfaces and glycine, isoleucine, and histi-

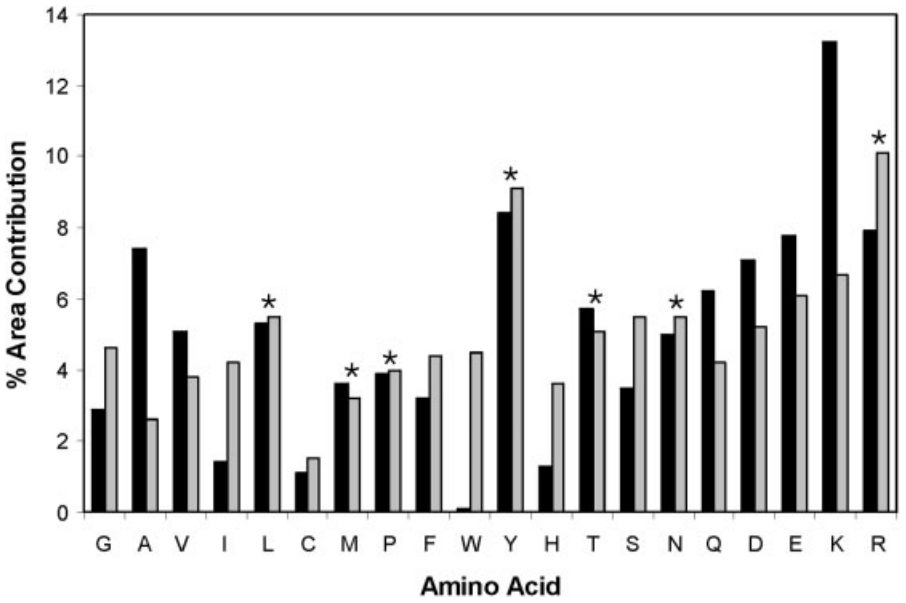

Fig. 1. (Black bars) A plot of the average percentage area contributions of individual amino acids to the interfaces found in redox protein complexes. The set of redox protein interfaces contains a total of 408 interface residues. (Gray bars) The results of Lo Conte et al.[13] are shown for comparison. (*) Residues that have similar percentage area contributions (within 20%) in the two sets of complexes are indicated.

dine, which are all less abundant in redox protein complexes. However, the most striking difference concerns tryptophan. Lo Conte et al.[13] found that tryptophan contributes 1.3 and 4.5% to the solvent ASA and the interface area, respectively. This corresponds to a more than threefold enrichment of this residue in the interface.[13] In contrast, only one of the redox protein complexes, *ami:madh*, has a tryptophan side chain in the interface. A sequence analysis of the homologues of *adx*, *fdx*, *ami*, *azu*, and *cytc* proteins was performed in order to test the significance of this result. It was found that the binding domains of these proteins rarely contain tryptophan. The only occurrence was in $cytc_2$ from *Agrobacter tumefaciens*, which has a tryptophan in place of the conserved K105 (a contributing residue in the $cytc_2$*:rc* interface).

Inspection of the crystal structures of redox protein complexes reveals that the core of the interface is composed of predominantly hydrophobic residues surrounding the redox active site. Representative examples of binding sites are illustrated in Figure 2, corresponding to four of the *cyt* complexes, the three complexes involving iron–sulfur proteins, and one of the cupredoxin complexes. Those atoms that lose ASA upon complex formation are colored. Atoms that make van der Waals contacts across the interface are also distinguished. With the exception of arginine (for reasons discussed later), there is a strong preference for charged groups to be located on the periphery of the binding site. Polar side chains also tend to occur on the periphery, although the preference is less pronounced. In some cases, threonine and serine are located closer to the center of the binding site. It should be noted, however, that the polar groups are often involved in intramolecular hydrogen bonds, reducing their availability for polar interactions across the interface. Figure 2 highlights the sparse distribution of contact atoms and the relative abundance of "holes," which are large areas within the binding site that remain solvent accessible. Furthermore, it highlights the flexibility of the binding sites employed in homologous complexes. Although similar regions of the protein are involved in the interfaces, the detailed architecture of the *fdx* [Fig. 2(B and C)] and the yeast *cytc* binding sites [Fig. 2(F and G)] is remarkably different.

Polar Interactions

Although all of the structure articles report the occurrence of hydrogen bonds and/or salt bridges in the complex interfaces, few of them have stated the criteria used for identifying such interactions. Therefore, in order to accurately compare the complexes, polar interactions were calculated using HBPLUS.[39] The results of these calculations are presented in Table II.

According to two studies by Thornton and coworkers, the average occurrence of polar interactions is approximately 1 hydrogen bond per 100 $Å^2$ of interface area.[9,15] In 36 structures of 2.4 Å resolution or higher, Lo Conte et al. found an average of one hydrogen bond per 170 $Å^2$.[13] (The difference in these two values is related to the definition of the interface area.[9,13]) None of the structures listed in Table II have a hydrogen bond density even approaching these values. With the exception of the *adx:adr* complex (1 H bond/230 $Å^2$), the occurrence of intermolecular hydrogen bonds is extremely limited. In fact, HBPLUS does not assign any polar interactions in four of the complexes. This may be chemically correct; however, it may also reflect the sensitivity of the calculation, because inaccuracies in the atomic coordinates can conceal the presence of hydrogen bonds.[13] The difference in the *fdx:fnr* complexes is also

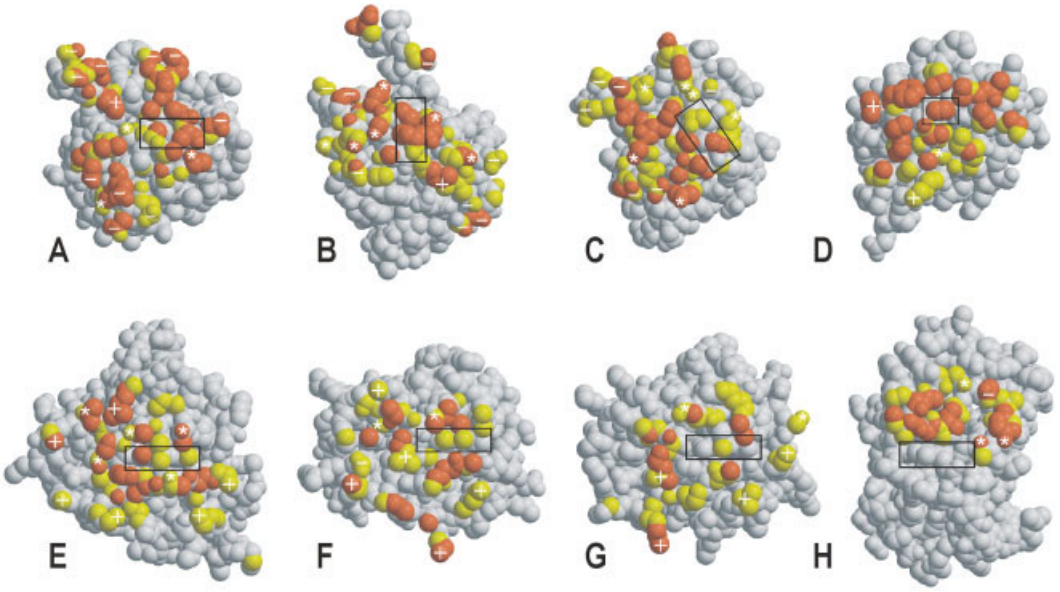

Fig. 2. The binding sites observed in the crystal structures of eight representative redox protein complexes: (**A**) *adx*,[19] (**B**) Mz *fdx*,[21] (**C**) Ab *fdx*,[23] (**D**) *ami* in *ami:madh*,[25] (**E**) $cytc_2$,[27] (**F**) *cytc* in *cytc:ccp*,[29] (**G**) *cytc* in $cytc{:}bc_1$,[35] and (**H**) $cytc_{551}$.[25] The structures are represented as space-filling models. (Yellow) Those atoms that lose solvent ASA in the interface and (orange) atoms that make van der Waals contacts across the interface are shown. The approximate location of charges is indicated by plus (+) and minus (−) signs; (*) the polar groups of threonine, serine, asparagine, glutamine, and tyrosine are noted. The location of heme groups and active-site residues is indicated by rectangular boxes. The figures were drawn in Molscript[72] and rendered in Raster3D.[73]

surprising. Despite the similar interface size, the number of polar interactions is calculated to be higher in the maize complex. Water molecules buried in the interface can mediate polar interactions.[13] For example, the interface of the *azu* dimer contains two well-defined water molecules, which connect the active site histidines via a network of 3 hydrogen bonds.[31]

Arginine is the only charged residue that is commonly found in the core of the interface in redox protein complexes. In addition to its hydrogen bonding capabilities, the arginine side chain can also participate in cation–π interactions with aromatic rings.[46] Four cation–π interactions were identified in the complex interfaces listed in Table II: two between arginine and phenylalanine (*ami:madh*, $cytc{:}bc_1$) and two between arginine and tyrosine side chains ($cytc_2{:}rc$, $ami{:}cytc_{551}$). With the exception of the *azu* dimer, all of the interfaces contain one or more arginine side chains, with as many as six involved in the *adx:adr* interface (Table III). Previous studies have highlighted the importance of arginine in complex interfaces. Bogan and Thorn have shown that arginine (along with tyrosine and tryptophan) is one of the most frequent "hot spot" residues, contributing ≥2 kcal/mol to the binding free energy.[12] Lo Conte et al. have demonstrated that arginine contributes the most surface to the interface area on average,[13] accounting for about 10% of the total (Fig. 1). It was found that tyrosine is equally prevalent in these interfaces. Similar values were obtained for arginine and tyrosine in the redox protein complexes analyzed in this work (Fig. 1). Furthermore, in eight of the complexes we found that either an arginine or tyrosine contributed the most surface area to the interface (Table II). This suggests that the binding sites of electron transfer proteins employ similar roles for these residues in terms of interfacial contacts and hot spots. Lysine, on the other hand, is twice as abundant in redox protein complexes (Fig. 1) compared with the results of Lo Conte et al.[13] The reason for this difference is discussed in the following section.

Electrostatics and Redox Protein Complexes

It has long been recognized that protein–protein association is influenced by electrostatic interactions.[47–49] The role of electrostatics in the formation of redox protein complexes has received support from several lines of evidence: the presence of complementary charged patches on partner proteins,[50] the strong ionic strength dependence of reaction rates,[26,51] covalent crosslinking using carbodiimide,[52] and tuning of the reaction rate via mutagenesis of charged residues.[53,54]

It can be concluded from these studies that Coulombic attraction is one of the driving forces behind the rapid association rates ($k_{on} > 10^8\ M^{-1}\ s^{-1}$) observed in electron transfer complexes. However, although electrostatics can accelerate and preorient protein association, the contribution to the binding affinity appears to be less favorable.[49] Experimental and theoretical studies indicate that the cost of dehydration of charged groups outweighs the contribution of salt bridges to the complex stability.[55,56] A detailed analysis of the binding sites provides a structural basis in support of this view of electrostatics. Table III lists the percentage area contribution of charged residues and the number of charged atoms (which lose ASA) in the

TABLE III. Percentage Area Contribution of Charged Residues and Formal Charge Content of Redox Protein Interfaces

	% Area Contribution[a]				Interface Charge[b]					
Complex	Asp	Glu	Lys	Arg	Asp	Glu	Lys	Arg	Density[c] (Å^2)	$E_{Coulomb}$[d] (kJ/mol)
adx	^{6}32	^{3}16	0	^{2}7	6	3	0	2	120	−28.8
adr	^{1}1	^{2}6	^{2}13	^{4}25	1	1	2	4		
Mz *fdx*	^{4}12	^{2}11	0	^{1}6	4	2	0	1	90	30.6
Mz *fnr*	^{1}2	^{3}13	^{8}41	^{1}1	1	3	7	1		
Ab *fdx*	^{5}27	^{1}3	0	^{1}2	5	1	0	0	110	12.4
Ab *fnr*	0	^{4}12	^{3}16	^{3}20	0	4	3	2		
ami	0	0	^{3}11	^{1}7	0	0	1	1	240	25.5
madh	^{2}9	^{1}9	^{1}1	^{1}6	2	1	0	1		
$cytc_2$	0	0	^{7}25	^{1}14	0	0	5	1	130	−16.4
rc	^{3}8	^{1}1	0	0	3	1	0	0		
cytc	^{1}2	0	^{6}35	^{1}12	1	0	4	1	105	−87.8
ccp	^{1}7	^{3}15	0	^{1}10	1	3	0	1		
hcytc	^{1}0	^{1}7	^{6}53	0	1	1	6	0	85	−82.0
ccp	^{1}8	^{3}21	0	^{1}12	1	2	0	1		
azu	^{1}4	0	0	0	1	0	0	0	500	5.7
azu	^{1}4	0	0	0	1	0	0	0		
etf	^{1}8	0	^{2}3	^{1}20	1	0	2	1	190	64.3
tmadh	^{1}2	^{1}1	^{3}12	0	1	0	0	0		
cytc	0	0	^{4}34	^{1}16	0	0	2	1	175	ND[e]
bc_1	^{1}6	^{1}13	0	^{1}1	1	1	0	0		
ami	^{1}9	^{2}32	^{2}21	^{1}7	1	2	1	1	140	38.6
$cytc_{551}$	^{1}14	^{1}4	^{1}12	0	1	0	0	0		
br	0	^{2}12	^{2}8	^{3}32	0	2	2	3	140	−18.8
*b**	^{2}26	^{3}8	0	0	2	2	0	0		

[a]The values are given as the percentage contribution per component of the interface with the number of contributing residues indicated in the superscript.
[b]The number of charges in the interface. Charges were assigned for those atoms that lose solvent accessible surface area. (ASA) in the interface. A unit charge was assigned when one or both acidic oxygens of aspartic acid or glutamic acid, the amino nitrogen of lysine, or one or both guanidyl nitrogens of arginine lose ASA.
[c]The charge density is given as the interface size (B) divided by the total number of charged groups present in the interface. It should be noted that charged groups are not evenly distributed but tend to occupy the periphery of the interface (see text).
[d]The intermolecular Coulomb energy was calculated for formal charges only.
[e]Not determined.

complex interface. With the exception of the *azu* dimer, charged atoms occur with a frequency of about one per 140 Å^2 of interface area. These data indicate that few charged groups contribute to the interface (see also Fig. 2) and even fewer are involved in salt bridges (Table II). Only the *adx:adr* complex has an appreciable quantity of charged groups; but, considering it has an interface that is 50% larger than that of the high-affinity *br:b** complex, the number of charge interactions is still relatively low. A calculation of the intermolecular Coulombic energy (formal charges only) was performed for each complex (Table III). Surprisingly, this energy term favors fast association in only four cases. It is particularly favorable for the *cytc:ccp* complex in agreement with the extremely fast k_{on} value ($\sim 10^{10}\ M^{-1}\ s^{-1}$) for this complex. The interaction of *fdx* and *fnr* also proceeds with a fast k_{on} value ($\sim 10^{8}\ M^{-1}\ s^{-1}$ for the *Anabaena* proteins[22]) and yet the Coulombic energy is calculated to be unfavorable. This suggests that, although electrostatic attraction can accelerate protein association, the Coulombic interaction is not necessarily optimized in the fully bound complex. The *azu:azu*, *ami:cytc*$_{551}$, and *etf:tmadh* complexes have low k_{on} values (10^5–$10^6\ M^{-1}\ s^{-1}$) and unfavorable Coulombic energies, which agrees with the poor electrostatic complementarity in these complexes (Table III). The Coulombic energy calculation is less informative in the *etf:tmadh* case, however, because the interface is incomplete.[33]

Although lysine residues contribute the most surface area on average to the interface (Fig. 1), this contribution is largely made up of the side-chain methylenes rather than the amino group itself. For example, the *hcytc* interface is 66% apolar (Table II) despite the fact that six lysine residues account for 53% of the interface area (Table III). Moreover, it should be noted that there were no occurrences of fully buried lysine N^{ζ} atoms in any of the redox protein complexes. The distribution of lysines on the periphery of the interface facilitates this effect. Similarly, the acidic side chains are found toward the extremities of the binding site (Fig. 2). Such an arrangement is preferable for association in the high-turnover regime because it guarantees fast, productive association between oppositely charged proteins. In a recent analysis of protein recognition sites, Chakrabarti and Janin found that certain amino acids have a preference for either the core or

TABLE IV. Atom Packing and Geometric Complementarity in Redox Protein Complexes

Complex	Interface atoms[a]	Buried atoms[b]		Water buried[c]		Gap Index[d] (Å)
		No.	V/V_0	No.	V'/V_0	
adx:adr	237	49	1.06	70	1.07	3.1
Mz *fdx:fnr*	186	19	1.04	—	—	4.9
Ab *fdx:fnr*	185	30	1.11	33	1.12	4.9
ami:madh	157	45	1.07	57	1.05	4.2
cytc$_2$:rc	129	35	1.11	59	1.08	7.4
cytc:ccp	113	14	1.04	42	1.09	4.5
hcytc:ccp	114	20	1.04	—	—	5.4
azu:azu	88	16	1.01	40	1.00	2.5
etf:tmadh	116	24	1.01	76	1.02	6.7
cytc:bc$_1$	109	7	1.06	—	—	ND[e]
ami:cytc$_{551}$	93	30	1.07	33	1.06	5.5
Mean[f]	139 (47)	26 (13)	1.06 (0.03)	51 (17)	1.06 (0.04)	4.9 (1.5)
*br:b**	185	50	1.00	111	1.00	1.7
LC Mean[g]	211 (81)	—	1.01 (0.02)	—	1.00 (0.02)	—

[a]The number of interface atoms, which lose ≥0.05 Å^2 surface area in the complex.
[b]Fully buried atoms (zero accessibility in the complex interface) are used to calculate the atom packing, V/V_0, where V is the Voronoi volume of buried atoms and V_0 is the reference volume.[41]
[c]When solvent molecules (in structures of 2.4 Å resolution or higher) are included, the number of fully buried atoms increases and the atom packing (V') can be recalculated.
[d]The gap volume index was calculated using Surfnet.[42]
[e]Not determined.
[f]The mean (standard deviation) as calculated for the 11 redox protein complexes.
[g]The mean (standard deviation) from the study by Lo Conte et al.[13] on a set of 75 protein complexes.

the rim of the interface.[14] In general, the rim of the interface has an amino acid composition with greater resemblance to the remainder of the protein surface whereas the core has a deficit in charged residues (except arginine). It was shown that although lysine and glutamic acid each contribute ~10% to the surface area of the rim, they account for only ~5% of the interface core. Moreover, these two residues had the lowest propensity to be found in the core of the interface.[14]

Atom Packing and Geometric Fitting in Interfaces

The atoms buried in protein interiors have on average smaller volumes than the equivalent atoms in crystals of amino acids. Therefore, it can be concluded that the atom packing in the protein interior is higher than in small molecule crystals.[40,57] The degree of atom packing provides a measure of the geometric complementarity or "goodness of fit" and has practical applications in the study of protein–protein interfaces.

Several methods have been developed for the calculation of atom volumes in proteins.[40,58–60] For the sake of comparison with the results of Lo Conte et al.,[13] we have used an identical implementation of the Voronoi procedure.[40,41] This method represents each atom by a polyhedron, the faces of which are constructed from planes placed perpendicularly to the interatomic vectors between the atom and its neighbors.[41] In the case of surface atoms, which are not completely surrounded, such a calculation is impossible. However, if the water structure is defined, the Voronoi polyhedron can be completed. The packing efficiency[41] of interface atoms can be determined by calculating the volume (V) of the Voronoi polyhedron and comparing it with the mean volume (V_0) occupied by equivalent atoms in the protein interior.[57] A V/V_0 ratio greater than unity implies that the interface is poorly packed compared to the interior, whereas a ratio less than unity implies increased packing.

The interfaces found in the 11 redox protein complexes consist of between 90 and 240 atoms (Table IV). A remarkably small number of these atoms are fully buried, with as few as 7 fully buried atoms in the *cytc:bc$_1$* complex. On average, only one-fifth of the interface atoms are fully buried compared to one-third in the study by Lo Conte et al.[13] The V/V_0 ratio was calculated for these atoms and the results are listed in Table IV. An average of 1.06 was obtained and two of the complexes had a V/V_0 ratio higher than the range obtained by Lo Conte and coworkers.[13] Thus, in contrast to standard protein complexes,[13] the interface in electron transfer complexes is poorly packed. The atom packing in the *etf:tmadh* complex is more similar to that found within the protein interior. However, this complex involves two-site binding of a well-defined anchor domain and a highly mobile redox domain, which could not be observed crystallographically.[33] It is likely, therefore, that the increased packing of the anchor is necessary to compensate for the absence of interface contacts at the redox site. In any case, the number of fully buried atoms is low and the finding that it is close packed can be considered insignificant.[13]

Eight of the structures of 2.4 Å resolution or higher contain coordinates for solvent molecules. When water molecules were used to complete the Voronoi polyhedra, the number of interface atoms that could be included in the calculation was increased twofold on average. In some cases, calculations incorporating solvent positions resulted in a significant decrease in the V/V_0 ratio, indicating that water molecules contribute to the packing of the interface. In the *cytc:ccp* and *etf:tmadh* interfaces the number of fully buried atoms increases substantially in the presence of water. Therefore, the increase in V/V_0 probably reflects an improvement in the accuracy of the calculation.[13]

The gap volume index provides an alternative measure of geometric complementarity in the complex interface.[9] In this approach, the gap index is calculated as the volume of cavities in the interface divided by the interface area.[42] The larger the gap index the poorer the geometric fitting. An average gap index of 4.7 (±1.5) Å was obtained for the redox protein complexes (Table IV). Compared with an average gap index of 2.5 (±1.0) Å for 27 protein complexes (including 10 enzyme–inhibitor complexes) analyzed by Jones and Thornton,[9] this suggests that the geometric fitting is considerably lower in redox complexes. This result compares favorably with the poor atomic packing of the interface as indicated by the Voronoi volume calculations. The lower gap index of the *azu* homodimer can be attributed to the highly planar binding site that facilitates packing in this symmetric complex.

Recently, Nooren and Thornton analyzed the interfaces in transient homodimers and transient heterodimers.[15] The mean gap index (2.8 Å) was found to be slightly larger than that in high affinity protein complexes (2.5 Å). Several of the transient complexes have gap indices similar to those found in redox protein complexes. In particular, the bovine β-lactoglobulin homodimer and the α subunit of rat G_i protein in complex with its RGS regulator each have gap indices of 5.3 Å. This low geometric complementarity is consistent with poor atom packing at the interface, as indicated by the V/V_0 ratios of 1.05 and 1.08 calculated for each complex (this work). However, these complexes represent an extreme in the two types of interfaces studied by Nooren and Thornton.[15] Furthermore, Lo Conte et al.[13] calculated a mean V/V_0 ratio of 1.02 (±0.02) in a set of 11 complexes of G-proteins and signal transduction proteins. Therefore, it can be concluded that, of the complexes studied thus far, only the redox protein complexes are consistently poorly packed.

Variable Binding Sites and Promiscuity

Brownian motion can, in principle, give rise to (aspecific) interactions between any two proteins.[47] The presence of complementary electrostatics promotes the formation of such an encounter complex. This preliminary stage of crude recognition can then evolve into a reactive complex under the guide of specific short-range interactions. Redox proteins are reactive toward multiple partners and therefore utilize binding sites that must accommodate a variety of molecular surfaces.[5,33,61] In some redox pairs, more than one binding site is available for complex formation.[30] This apparent complexity of redox protein recognition is greatly simplified by the architecture of the binding site. The formation of poorly packed hydrophobic interfaces with low geometric complementarity enables the promiscuity of such interactions. Recent evidence also points to the existence of "dynamic ensembles" in that the partner proteins react without the formation of a well-defined complex. In these cases, it appears that there is insufficient hydrophobic-contact information to specify a single orientation.[62–64]

Several of the complexes analyzed in this study provide evidence of variable binding sites. In particular, different binding orientations are observed in the homologous peroxidase complexes[29] and *fdx:fnr* complexes[21,23] [Fig. 2(B and C)]. Furthermore, it was found that the chemical composition of the binding site can be significantly different depending on the complex, for example, compare yeast *cytc* in complex with *ccp* and bc_1 (see tables). Cocrystallization is subject to the constraints of the crystal lattice, and the lowest free energy packing within the crystal need not necessarily correspond to the optimal geometry of the native complex. Although this is particularly true for low affinity interactions, the binding sites observed by crystallography are in agreement with the results of NMR studies of transient complexes in solution. To date, complexes involving iron–sulfur proteins,[21,63,65] cytochromes,[28,65–68] and cupredoxins[44,45,69] have been observed and characterized by heteronuclear NMR. In the majority of these cases chemical-shift perturbation studies have revealed predominantly hydrophobic interfaces with polar or charged residues on the periphery of the binding site.[4] It has also been concluded from these investigations that redox protein interfaces have low geometric complementarity.[4,64,69]

Although few structures of redox protein complexes have been solved to date, the composition of the typical binding site is likely to be well represented by the data set analyzed in this article. This assumption is supported by the fact that similar features were observed in the three classes of metalloproteins. In addition, computational analyses of cupredoxins revealed a remarkable conservation of the hydrophobic patch in this extensive protein family.[43] Although the electrostatic properties can vary (depending on the subfamily and the organism), the charged residues are always located on the periphery of the hydrophobic patch.[43] Depending on the growth conditions, some organisms can utilize alternate redox carriers. These proteins (the plastocyanin/cytochrome c_6[70] and ferredoxin/flavodoxin[71] pairs) have been shown to have equivalent hydrophobic and charge distributions despite having very different primary, secondary, and tertiary structures. This suggests that the general features of redox protein binding sites are well conserved.

CONCLUSION

It has been shown that the interfaces in redox protein complexes are poorly packed and have low geometric fitting. Although lysine and the acidic residues are abundant in such interfaces, the charged groups are oriented

toward the periphery and rarely participate in hydrogen bonds or salt bridges. The core of the interface consists of a patch of hydrophobic side chains surrounding exposed ligands of the redox site or the heme edge in the case of cytochromes.

Poorly packed interfaces present two advantages in the arena of transient protein interactions. In the absence of strict geometric complementarity, protein binding becomes more flexible and facilitates interactions between a variety of partners. Furthermore, the process of dissociation, which involves solvation of the binding site, can proceed more rapidly when water molecules have increased access. Therefore, poorly packed interfaces can promote the fast k_{off}, which is essential for the transient interaction.

ACKNOWLEDGMENTS

The first author (P.B.C.) gratefully acknowledges funding from the Marie Curie Foundation under the Fifth Framework Programme. Dr. C.M. Soares is kindly recognized for providing a script to calculate the Coulomb interaction energies and for critically reading the manuscript.

REFERENCES

1. Mathews FS, Mauk AG, Moore GR. Protein–protein complexes formed by electron transfer proteins. In: Kleanthous C, editor. Protein–protein recognition. New York: Oxford University Press; 2000. p 60–101.
2. Schreiber G, Fersht AR. Interaction of barnase with its polypeptide inhibitor barstar studied by protein engineering. Biochemistry 1993;32:5145–5150.
3. Bendall DS. Interprotein electron transfer. In: Bendall DS, editor. Protein electron transfer. Oxford, UK: Bios Scientific; 1996. p 43–68.
4. Crowley PB, Ubbink M. Close encounters of the transient kind: redox protein interactions in the photosynthetic redox chain investigated by NMR spectroscopy. Acc Chem Res 2003;36:723–730.
5. McLendon G. Control of biological electron transport via molecular recognition and binding—the velcro model. Struct Bond 1991; 75:159–174.
6. Chothia C, Janin J. Principles of protein–protein recognition. Nature 1975;256:705–708.
7. Janin J, Chothia C. The structure of protein–protein recognition sites. J Biol Chem 1990;265:16027–16030.
8. Janin J. Principles of protein–protein recognition from structure to thermodynamics. Biochimie 1995;77:497–505.
9. Jones S, Thornton JM. Principles of protein–protein interactions. Proc Natl Acad Sci USA 1996;93:13–20.
10. Jones S, Thornton JM. Analysis of protein–protein interaction sites using surface patches. J Mol Biol 1997;272:121–132.
11. Tsai CJ, Lin SL, Wolfson HJ, Nussinov R. Studies of protein–protein interfaces: a statistical analysis of the hydrophobic effect. Protein Sci 1997;6:1426–1437.
12. Bogan AA, Thorn KS. Anatomy of hot spots in protein interfaces. J Mol Biol 1998;280:1–9.
13. Lo Conte L, Chothia C, Janin J. The atomic structure of protein–protein recognition sites. J Mol Biol 1999;285:2177–2198.
14. Chakrabarti P, Janin J. Dissecting protein–protein recognition sites. Proteins 2002;47:334–343.
15. Nooren IMA, Thornton JM. Structural characterisation and functional significance of transient protein–protein interactions. J Mol Biol 2003;325:991–1018.
16. Berman HM, Westbrook J, Feng Z, Gilliland G, Bhat TN, Weissig H, Shindyalov IN, Bourne PE. The Protein Data Bank. Nucleic Acids Res 2000;28:235–242.
17. Wodak SJ, Janin J. Structural basis of macromolecular recognition. Adv Protein Chem 2003;61:9–73.
18. Lambeth JD, Kamin H. Adrenodoxin reductase–adrenodoxin complex—flavin to iron–sulfur electron transfer as the rate limiting step in the NADPH cytochrome *c* reductase reaction. J Biol Chem 1979;254:2766–2774.
19. Müller JJ, Lapko A, Bourenkov G, Ruckpaul K, Heinemann U. Adrenodoxin reductase–adrenodoxin complex structure suggests electron transfer path in steroid biosynthesis. J Biol Chem 2001;276:2786–2789.
20. Onda Y, Matsumura T, Kimata-Ariga Y, Sakakibara H, Sugiyama T, Hase T. Differential interaction of maize root ferredoxin: NADP(+) oxidoreductase with photosynthetic and non-photosynthetic ferredoxin isoproteins. Plant Physiol 2000;123:1037–1045.
21. Kurisu G, Kusunoki M, Katoh E, Yamazaki T, Teshima K, Onda Y, Kimata-Ariga Y, Hase T. Structure of the electron transfer complex between ferredoxin and ferredoxin–NADP(+) reductase. Nature Struct Biol 2001;8:117–121.
22. Hurley JK, Fillat MF, Gomez-Moreno C, Tollin G. Electrostatic and hydrophobic interactions during complex formation and electron transfer in the ferredoxin–ferredoxin:NADP(+) reductase system from *Anabaena*. J Am Chem Soc 1996;118:5526–5531.
23. Morales R, Charon MH, Kachalova G, Serre L, Medina M, Gomez-Moreno C, Frey M. A redox-dependent interaction between two electron-transfer partners involved in photosynthesis. Embo Rep 2000;1:271–276.
24. Brooks HB, Davidson VL. Kinetic and thermodynamic analysis of a physiological intermolecular electron-transfer reaction between methylamine dehydrogenase and amicyanin. Biochemistry 1994; 33:5696–5701.
25. Chen LY, Durley RCE, Mathews FS, Davidson VL. Structure of an electron-transfer complex—methylamine dehydrogenase, amicyanin and cytochrome c_{551}. Science 1994;264:86–90.
26. Moser CC, Dutton PL. Cytochrome *c* and cytochrome c_2 binding-dynamics and electron-transfer with photosynthetic reaction center and other integral membrane redox proteins. Biochemistry 1988;27:2450–2461.
27. Axelrod HL, Abresch EC, Okamura MY, Yeh AP, Rees DC, Feher G. X-ray structure determination of the cytochrome c_2: reaction center electron transfer complex from *Rhodobacter sphaeroides*. J Mol Biol 2002;319:501–515.
28. Worrall JAR, Kolczak U, Canters GW, Ubbink M. Interaction of yeast iso-1-cytochrome *c* with cytochrome *c* peroxidase investigated by [N-15,H-1] heteronuclear NMR spectroscopy. Biochemistry 2001;40:7069–7076.
29. Pelletier H, Kraut J. Crystal structure of a complex between electron-transfer partners, cytochrome *c* peroxidase and cytochrome *c*. Science 1992;258:1748–1755.
30. Zhou JS, Hoffman BM. Stern–Volmer in reverse—2:1 stoichiometry of the cytochrome *c*–cytochrome *c* peroxidase electron transfer complex. Science 1994;265:1693–1696.
31. van Amsterdam IMC, Ubbink M, Einsle O, Messerschmidt A, Merli A, Cavazzini D, Rossi GL, Canters GW. Dramatic modulation of electron transfer in protein complexes by cross-linking. Nature Struct Biol 2002;9:48–52.
32. Wilson EK, Scrutton NS, Colfen H, Harding SE, Jacobsen MP, Winzor DJ. An ultracentrifugal approach to quantitative characterization of the molecular assembly of a physiological electron-transfer complex—the interaction of electron-transferring flavoprotein with trimethylamine dehydrogenase. Eur J Biochem 1997;243: 393–399.
33. Leys D, Basran J, Talfournier F, Sutcliffe MJ, Scrutton NS. Extensive conformational sampling in a ternary electron transfer complex. Nature Struct Biol 2003;10:219–225.
34. Speck SH, Margoliash E. Characterization of the interaction of cytochrome *c* and mitochondrial ubiquinol–cytochrome *c* reductase. J Biol Chem 1984;259:1064–1072.
35. Lange C, Hunte C. Crystal structure of the yeast cytochrome bc_1 complex with its bound substrate cytochrome *c*. Proc Natl Acad Sci USA 2002;99:2800–2805.
36. Davidson VL, Jones LH. Electron transfer from copper to heme within the methylamine dehydrogenase–amicyanin–cytochrome c_{551i} complex. Biochemistry 1996;35:8120–8125.
37. Buckle AM, Schreiber G, Fersht AR. Protein–protein recognition—crystal structural analysis of a barnase barstar complex at 2.0 Å resolution. Biochemistry 1994;33:8878–8889.
38. Hubbard SJ, Campbell SF, Thornton JM. Molecular recognition—conformational analysis of limited proteolytic sites and serine proteinase protein inhibitors. J Mol Biol 1991;220:507–530.

39. McDonald IK, Thornton JM. Satisfying hydrogen bonding potentials in proteins. J Mol Biol 1994;238:777–793.
40. Richards FM. Interpretation of protein structures—total volume, group volume distributions and packing density. J Mol Biol 1974;82:1–14.
41. Gerstein M, Tsai J, Levitt M. The volume of atoms on the protein surface: calculated from simulation, using Voronoi polyhedra. J Mol Biol 1995;249:955–966.
42. Laskowski RA. Surfnet—a program for visualizing molecular surfaces, cavities and intermolecular interactions. J Mol Graphics 1995;13:323–330.
43. De Rienzo F, Gabdoulline RR, Menziani MC, Wade RC. Blue copper proteins: a comparative analysis of their molecular interaction properties. Protein Sci 2000;9:1439–1454.
44. Ubbink M, Ejdebäck M, Karlsson BG, Bendall DS. The structure of the complex of plastocyanin and cytochrome *f*, determined by paramagnetic NMR and restrained rigid-body molecular dynamics. Structure 1998;6:323–335.
45. Crowley PB, Otting G, Schlarb-Ridley BG, Canters GW, Ubbink M. Hydrophobic interactions in a cyanobacterial plastocyanin–cytochrome *f* complex. J Am Chem Soc 2001;123:10444–10453.
46. Mitchell JBO, Nandi CL, McDonald IK, Thornton JM, Price SL. Amino–aromatic interactions in proteins—is the evidence stacked against hydrogen bonding? J Mol Biol 1994;235:315–331.
47. Berg OG, von Hippel PH. Diffusion controlled macromolecular interactions. Annu Rev Biophys Biophys Chem 1985;14:131–160.
48. Janin J. The kinetics of protein–protein recognition. Proteins 1997;28:153–161.
49. Sheinerman FB, Norel R, Honig B. Electrostatic aspects of protein–protein interactions. Curr Opin Struct Biol 2000;10:153–159.
50. Koppenol WH, Margoliash E. The asymmetric distribution of charges on the surface of horse cytochrome *c*—functional implications. J Biol Chem 1982;257:4426–4437.
51. Simondsen RP, Weber PC, Salemme FR, Tollin G. Transient kinetics of electron transfer reactions of flavodoxin—ionic strength dependence of semi-quinone oxidation by cytochrome *c*, ferricyanide and ferric ethylenediaminetetracetic acid and computer modeling of reaction complexes. Biochemistry 1982;21:6366–6375.
52. Moench SJ, Satterlee JD, Erman JE. Proton NMR and electrophoretic studies of the covalent complex formed by cross-linking yeast cytochrome *c* peroxidase and horse cytochrome *c* with a water-soluble carbodiimide. Biochemistry 1987;26:3821–3826.
53. Caffrey MS, Bartsch RG, Cusanovich MA. Study of the cytochrome c_2–reaction center interaction by site directed mutagenesis. J Biol Chem 1992;267:6317–6321.
54. Kannt A, Young S, Bendall DS. The role of acidic residues of plastocyanin in its interaction with cytochrome *f*. BBA-Bioenergetics 1996;1277:115–126.
55. Waldburger CD, Schildbach JF, Sauer RT. Are buried salt-bridges important for protein stability and conformational specificity? Nature Struct Biol 1995;2:122–128.
56. Elcock AH, Gabdoulline RR, Wade RC, McCammon JA. Computer simulation of protein–protein association kinetics: acetylcholinesterase–fasciculin. J Mol Biol 1999;291:149–162.
57. Tsai J, Taylor R, Chothia C, Gerstein M. The packing density in proteins: standard radii and volumes. J Mol Biol 1999;290:253–266.
58. Connolly ML. Computation of molecular volume. J Am Chem Soc 1985;107:1118–1124.
59. Pattabiraman N, Ward KB, Fleming PJ. Occluded molecular surface: analysis of protein packing. J Mol Recognit 1995;8:334–344.
60. Word JM, Lovell SC, La Bean TH, Taylor HC, Zalis ME, Presley BK, Richardson JS, Richardson DC. Visualizing and quantifying molecular goodness-of-fit: small-probe contact dots with explicit hydrogen atoms. J Mol Biol 1999;285:1711–1733.
61. Pettigrew GW, Moore GR. Cytochromes *c*: biological aspects. New York: Springer–Verlag; 1987.
62. Liang ZX, Nocek JM, Huang K, Hayes RT, Kurnikov IV, Beratan DN, Hoffman BM. Dynamic docking and electron transfer between Zn-myoglobin and cytochrome b_5. J Am Chem Soc 2002;124:6849–6859.
63. Worrall JAR, Liu Y, Crowley PB, Nocek JM, Hoffman BM, Ubbink M. Myoglobin and cytochrome b_5: a nuclear magnetic resonance study of a highly dynamic protein complex. Biochemistry 2002;41:11721–11730.
64. Worrall JAR, Reinle W, Bernhardt R, Ubbink M. Transient protein interactions studied by NMR spectroscopy: the case of cytochrome *c* and adrenodoxin. Biochemistry 2003;42:7068–7076.
65. Morelli X, Dolla A, Czjzek M, Palma PN, Blasco F, Krippahl L, Moura JJG, Guerlesquin F. Heteronuclear NMR and soft docking: an experimental approach for a structural model of the cytochrome c_{553}–ferredoxin complex. Biochemistry 2000;39:2530–2537.
66. Crowley PB, Rabe KS, Worrall JAR, Canters GW, Ubbink M. The ternary complex of cytochrome *f* and cytochrome *c*: identification of a second binding site and competition for plastocyanin binding. ChemBioChem 2002;3:526–533.
67. Crowley PB, Díaz-Quintana A, Molina-Heredia FP, Nieto P, Sutter M, Haehnel W, De la Rosa MA, Ubbink M. The interactions of cyanobacterial cytochrome c_6 and cytochrome *f*, characterized by NMR. J Biol Chem 2002;277:48685–48689.
68. Wienk H, Maneg O, Lucke C, Pristovsek P, Lohr F, Ludwig B, Ruterjans H. Interaction of cytochrome *c* with cytochrome *c* oxidase: an NMR study on two soluble fragments derived from *Paracoccus denitrificans*. Biochemistry 2003;42:6005–6012.
69. Crowley PB, Vintonenko N, Bullerjahn GS, Ubbink M. Plastocyanin–cytochrome *f* interactions: the influence of hydrophobic patch mutations studied by NMR spectroscopy. Biochemistry 2002;41:15698–15705.
70. Frazão C, Soares CM, Carrondo MA, Pohl E, Dauter Z, Wilson KS, Hérvas M, Navarro JA, De la Rosa MA, Sheldrick GM. Ab-initio determination of the crystal structure of cytochrome c_6 and comparison with plastocyanin. Structure 1995;3:1159–1169.
71. Ullmann GM, Hauswald M, Jensen A, Knapp EW. Structural alignment of ferredoxin and flavodoxin based on electrostatic potentials: implications for their interactions with photosystem I and ferredoxin–NADP reductase. Proteins 2000;38:301–309.
72. Kraulis PJ. MOLSCRIPT—a program to produce both detailed and schematic plots of protein structures. J Appl Crystallogr 1991;24:946–950.
73. Merritt EA, Bacon DJ. Raster3D: photorealistic molecular graphics. Methods Enzymol 1997;277:505–524.